DEVELOPMENT AND PERFORMANCE EVALUATION OF TUMOR TARGETING POTENTIAL OF FOLATE SPACER FUNCTIONALIZED SOLID LIPID NANOPARTICLES

SHIKHA SINGH*, PRIYANKA CHATURVEDI, SURENDRA K JAIN

Department of Pharmacy, Sagar Institute of Research and Technology Pharmacy, Bhopal, Madhya Pradesh, India. Email: shikha.aips@gmail.com

ABSTRACT

Objective: The objective of the present investigation was to assess the tumor-targeting potential of ligand-spacer engineered solid lipid nanoparticles (SLN) as nanoscale drug delivery units for site-specific delivery of a model anticancer agent, paclitaxel (PTX). SLNs were engineered by direct and indirect conjugation of folic acid (FA) through different types of polyethylene glycols (PEGs) (MW: 1000, 4000) as spacers.

Methods: The synthesized nanoconjugates (SLNFA, SLN1FA, and SLN4FA) were characterized by Fourier transform infrared spectroscopy, nuclear magnetic resonance, and transmission electron microscopic studies. Nanoconjugates were evaluated for entrapment, *in vitro* drug release (under various pH conditions) and hemolytic studies. Cell uptake and cytotoxicity studies were performed on human malignant cell lines (MCF-7) using 3-(4,5-dimethylthiazol-2-yl)-2,5-diphenyltetrazolium bromide assay.

Results: This study explored the effect of PEG spacer length on the targeting potential of folate-conjugated SLN. PTX entrapment and *in vitro* drug release from nanoconjugates augmented, and hemolytic toxicity of nanoconjugates slashed with the molecular weight of PEGs. Further, nanoconjugates with PEG 4000 displayed highest tumor-targeting potential as compared to other spacer conjugated nanoconjugates due to optimized steric hindrance and receptor mediated endocytosis among other PEGs.

Conclusion: Engineering of the dendritic surface with targeting ligand such as FA can enhance the site-specific anticancer drug delivery. PEGylation of SLN can improve the circulation time of SLN in the body. This is a debut study reporting FA conjugation to the surface through four PEGs as spacer and optimized the spacer chain length for effective cancer targeting through SLN. This report as a whole is believed to shed new light on the role of spacer chain length in targeting potential of folate-anchored SLN.

Keywords: PEGylation, Targeting, Solid lipid nanoparticles, Hemolytic toxicity, Cytotoxicity, Cancer, Polyethylene glycols as spacer.

INTRODUCTION

According to the global cancer report issued by the 48 World Health Organization (WHO), cancer is the leading cause of death in economically developed countries and the second leading cause of death in developing countries, and deaths from cancer worldwide are projected to continue rising, with an estimated 12 million deaths in 2030 [1]. Although there has been potential progress in the prevention, detection, and treatment of cancer over the past 50 years adequate therapy remains elusive due to late stage diagnosis, inadequate strategies for addressing aggressive metastasis, and lack of clinical procedures for overcoming multidrug-resistant (MDR) cancer [2,3]. MDR can be intrinsic (inherent) or acquired through chemotherapy exposure [4]. The development of MDR contributes to the persistence of the disease in spite of high dose and combination chemotherapy, which is often the last treatment option [5]. However, this often leads to toxic side effects and poor clinical outcomes. The majority of clinically approved chemo 68 motherapeutic agents target cell growth patterns and are not selective for cancer cells [6]. Nanotechnology offers an unprecedented opportunity in rational delivery of drugs and genes to solid tumors [7] following systemic administration due to their unique accumulation behavior at the tumor site [8,9]. Examples of nanotechnology applied in pharmaceutical product development include nanoparticles, dendrimers, and liposomes [10]. Targeted anticancer drug delivery includes drug delivery by avoiding reticuloendothelial system 80 (RES) [11], utilizing the enhanced permeability and retention effect and tumor specific targeting [12]. Nanoparticles made from solid lipids are attained major attraction as novel drug carrier for intravenous and nasal application as they have been proposed as an alternative particulate carrier system [13]. The solid lipid nanoparticles (SLNs) are sub-micron colloidal carriers (50–1000 nm), which are composed of physiological lipid dispersed in water or in an aqueous surfactant solution [14]. SLNs as colloidal carriers for drugs combine the advantage of polymeric nanoparticles, fat emulsions and liposomes simultaneously and avoiding some of their disadvantages [15]. They have been widely used for controlled drug delivery through intravenous, transdermal, ocular, and oral administration routes. The first study on SLNs for paclitaxel (PTX) delivery was reported by Miglietta *et al.* in 2000 [16]. Developed tripalmitin-based SLNs stabilized by soya phosphatidylcholine, with average diameter below 500 nm, with proven stability in isotonic glycerol solution. Encapsulation or conjugation of bioactive molecules in these functional solid lipid nanoparticles may reduce their toxicity, enhance their solubility, and prolong blood clearance. PEGylation is effective approach for drug delivery because of the escape from the recognition by the RES. Different types of PEGylated solid lipid nanoparticles using polyvinyl chloride have already been reported. Recently, conjugation of targeting ligand through polyethylene glycols (PEG) as spacer considered as most potential approach to improve the targeting properties of SLNs was synthesized folate PEG-modified SLNs nanoconjugates as a drug delivery system. The role of PEG chains as spacer show important potential with targeting ligand employed for the functionalization of surface groups [17]. Thus, PEG enhances targeting in addition to enhancing solubilization of bioactive and reducing immunogenicity and toxicity of the carrier, which is a property of critical importance for drug delivery systems [18]. Furthermore, the introduction of a folate group at the end of PEG chains conjugated to solid lipid nanoparticles induces tumor-targeting potential to the carrier due to its receptor mediated endocytosis. Folate as ligand for tumor targeting has already applied with liposomes, nanoparticles, and dendrimers 137 Folate-based cancer targeting is an established

concept and solid lipid nanoparticles have been widely explored for targeting employing folate as ligand [19]. In this line, different reports on usage of various PEGs as spacer are available but effect of spacer chain length on targeting potential is lacking. Furthermore, the importance of spacer in cancer targeting has been well accepted. Steric hindrance as well as ligand presentation is believed to be a pre-requisite to achieve ligand receptor-based cancer targeting [19]. The purpose of the present investigation was to compare the tumor-targeting potential of ligand and ligand-spacer-engineered solid lipid nanoparticles nanoconju1gates as nanoscale drug delivery units for site-specific delivery of a model anticancer agent, Paclitaxel 1 (PTX). In the present study, SLN- spacer-folate nanoconjugates were synthesized with PEGs (Mw: 1000, 4000) which in addition to the protection exercised by the PEGs chains was also functionalized by a folate targeting ligand at the end of the one PEG chain with each nanoconjugates. In this manner, the folate group, due to its location at the distal end of PEG chain, is accessible to interact with complementary receptor. In addition, a folate-SLN nanoconjugate has also been synthesized to be used as a control to compare the tumor-targeting potential of synthesized nanoconjugates [20]. This work is expected to throw new light on the role of spacer chain length in targeting potential of folate-anchored SLNs [21].

MATERIALS AND METHODS

Materials
PTX was received gift sample from Sun Pharmaceutical Industries Ltd, Gujarat, (India). Soya Phosphatidyl Choline was purchased from HiMedia. Reagents and solvents analytical grade were purchased from local suppliers unless stated otherwise. Deionized water was used throughout the study.

Preparation of SLNs
Preparation of plain SLNs was carried out employing solvent injection method, which involves the rapid diffusion of solvent across the solvent-lipid phase into the aqueous phase. Tristearin, PC, stearylamine, and drug were dissolved in ethanol, maintained at an elevated temperature of 70°C with continuous stirring. This solution was injected into an aqueous solution of Tween 80 maintained at the same temperature given above with continuous stirring and sonicated under probe sonicator. The prepared nanoparticulate formulation was optimized for various parameters such as lipid lecithin ratio, drug-lipid ratio, surfactant ratio, stirring time, stirring speed, and sonication time to obtain nanosized SLNs with maximum drug entrapment. Lipid employed in the production of SLNs was first subjected to optimization by varying the ratio of tristearin: PC from 1:0.5 to 1:2, keeping tristearin quantity as constant [22,23] Tables 1 and 2.

$L_3D_2A_2S_2P_3T_3$ J, where, L = Lipid/Lecithin ratio; A = Lipid Stearylamine ratio; S = Concentration of tween 80; D = Drug P = RPM (stirring speed); T = Stirring time; J = Sonication time.

Synthesis of SLNs nanoconjugate
Various SLN based folate anchored nanoconjugates (SLN-Folate [SLNFA], SLN-PEG1000-Folate [SLNP1FA], and SLN-PEG4000-Folate [SLNP4FA]) wherein folic acid (FA) is attached directly or indirectly through different types of PEGs (1000/4000) as spacers; were synthesized using the stepwise typical conjugation chemistry of 1-Ethyl-3-[3-dimethylaminopropyl] carbodiimide (EDC), N-hydroxysuccinimide (NHS) dicyclohexylcarbodiimide (DCC), 4-Dimethylaminopyridine (DMAP), and 1,1'-Carbonyldiimidazole

(CDI). This debut study is described in detail through Scheme 1 and 2 (a and b). All synthesized nanoconjugates with conjugating agents. The conjugation of FA on SLN was accomplished using two methods; by direct conjugation on periphery and through different PEGs as spacer effect of conjugation on the absorption maxima of SLNs is described in Alshubaily *et al.* [20].

CHARACTERIZATION OF THE NANOCONJUGATES

Determination of drug content and entrapment efficiency
Drug entrapment of the PTX in SLNs was determined by dispersing the known molar concentration of PTX loaded SLNs in cellulose dialysis bag (MWCO 1000 Da, Sigma, Germany). This solution was dialyzed with the help of magnetic stirring (50 rpm; Remi, Mumbai, India) in cellulose dialysis bag against PBS (pH 7.4) under sink condition for 10 min to remove any unentrapped drug from the formulation. One milliliter aliquot was withdrawn and diluted 10 times in a volumetric flask with 30:70 methanols: PBS (pH 7.4). Absorbance was measured spectrophotometrically (Shimadzu, 1800 Japan) at 237 nm to indirectly estimate the amount of drug entrapped within the system. The dialyzed formulation was then lyophilized and further characterized. The amount of drug entrapped in folate coupled SLNs was also determined by employing the similar procedure as reported for PTX loaded SLNs [24].

Particle size determination
The average particle size and size distribution of the SLNs were determined by photon correlation spectroscopy using a Zetasizer DTS ver. 4.10 (Malvern Instrument, UK). The samples of SLN dispersions were diluted to 1:9 v/v with deionized water. The particles size and size distribution were represented by average (diameter) of the Gaussian distribution function in the logarithmic axis mode [25] (Table 3).
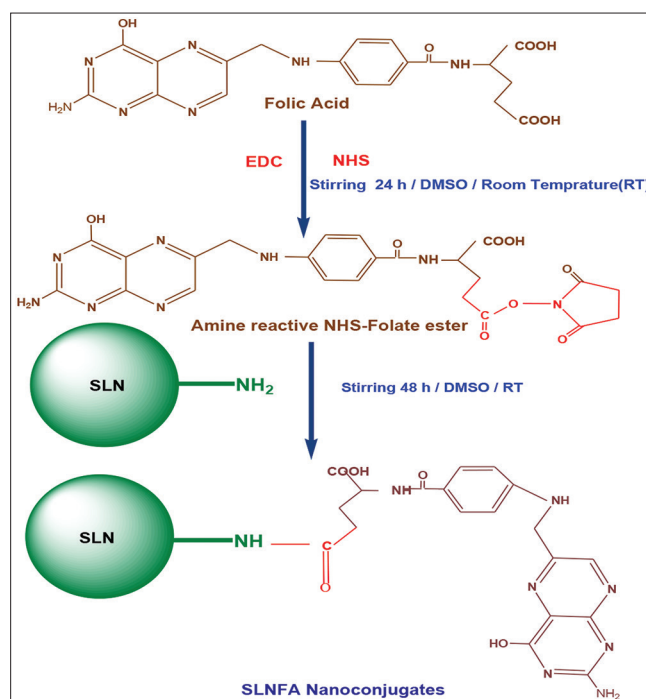
Scheme 1: Synthesis of SLNFA nanoconjugates

Table 1: Optimization batches ratio

S. No.	Formulation Code	Tristearin/Soya Lecithin Ratio% w/w	Lipid/SARatio (mg)	Tween80 Concentration (%w/v)	Drug/Lipid Ratio % w/w	Stirring speed (rpm)	Sonication time (min)
1.	$L_3A_2S_2D_2P_3T_3$ I	1.0 : 0.5	100: 0.5	0.5	5.0 : 100	~1000	1.0
2.	$L_3A_2S_2D_2P_3T_3$ J	1.0 : 1.0	100:1.0	1.0	10.0 : 100	~2000	2.0
3.	$L_3A_2S_2D_2P_3T_3$ K	1.5 : 1.0	100:1.5	1.5	15.0 : 100	~3000	3.0
4.	$L_3A_2S_2D_2P_3T_3$ L	2.0 : 1.5	100:2.0	2.0	20.0 : 100	~4000	4.0

Surface charge measurement

The surface charge of SLN was determined by measurement of zeta potential (ε) of the lipid nanoparticles calculated according to Helmholtz-Smoluchowsky from their electrophoretic mobility. For measurement of zeta potential, Zetasizer DTS ver 4.10 (Malvern Instrument, UK) was used. The field strength was 20 V/cm on a large bore measures cell. Samples were diluted with double-distilled water adjusted to a conductivity of 50 μS/cm with a solution of 0.9% NaCl.

Infrared (IR) spectroscopy

Synthesized nanoconjugates (SLNFA, SLNP1FA, and SLNP4FA) were characterized by Fourier-transform IR (FT-IR) spectroscopic technique using Nujol's mull method Elmer 783 Spectrophotometer. Various characteristic peaks in FT-IR spectrum were interpreted for different groups [26] (Fig. 1).

Particle morphology (transmission electron microscope [TEM])

TEM was used as a visualizing aid for particle morphology. The sample (10 μL) was placed on the grids and allowed to stand at room temperature for 90 s. Excess fluid was removed by touching the edge with filter paper. All samples were examined under a TEM (Philips

Morgagni 268, Eindhoven, Netherlands) at an acceleration voltage of 100 kV, and photomicrograph [27].

Microscopic study

Microscopic study of synthesized nanoconjugates SLNFA, SLNP1FA, and SLNP4FA was performed to characterize their size. TEM of the prepared nanoconjugates was done to characterize the systems after drying on 3 mm form an (0.5% plastic powder in amyl acetate) coated copper grid (300 mesh) at 60 KV (Philips Morgani, 268D; TEM [26], Holland) after staining negatively using uranyl acetate (4%) and photomicrographs were taken at suitable magnifications at Electron Microscopy Section of AIMS, Delhi (Fig. 3).

Nuclear magnetic resonance (^{1}H NMR) spectroscopy

The synthesized nanoconjugates SLNFA, SLNP1FA, and SLNP4FA were analyzed by ^{1}H NMR spectroscopy at NIPER, Hyderabad. The nanoconjugates were solubilized in D_2O and analyzed at 300 MHz by ^{1}H NMR Spectrometer model Avance-II (Bruker, Germany). Various shifts and peaks were observed, which were interpreted for different groups (Fig. 2).

***In vitro* drug release studies**

In vitro drug release profile of entrapped PTX from SLNs, SLNFA, SLNP1FA, and SLNP4FA was studied using dialysis tube. The SLN formulations were first separated from free drug by passing through sephadex G-50 column. The separated SLN formulation (5 ml) was taken in to dialysis tube (molecular weight cutoff 10,000 Da) and placed in a beaker containing 100 ml of phosphate buffer (pH 7.4). The beaker was placed over a magnetic stirrer and the temperature of the assembly was maintained at 37±1°C throughout the study. Samples were withdrawn at definite time intervals with replacement by same volume of phosphate buffer. The withdrawn samples were analyzed for

Table 2: Best Optimized Parameter of Optimized Formulation ($L_3A_2S_2D_2P_3T_3J$)

S. No.	Parameter	Optimized value
1.	Tristearin: Soya lecithin ratio	1.5: 1.0
2.	Drug: Lipid ratio	10:100 mg
3.	Surfactant concentration	1% w/v
4.	Stirring time	60 min
5.	Stirring speed	~3000 rpm
6.	Sonication time	2 min

Table 3: Particle size drug content and entrapment efficiency

S. No.	Formulation code	Particle size (nm)	Polydispersity index	%Drug entrapped
1.	PlainSLNs($L_3D_2A_2S_2P_3T_3J$)(SLN)	201.1±3.7	0.234	31.09±0.71
2.	Folate coupled SLNs ($L_3D_2A_2S_2P_3T_3JL_2$)(SLNFA)	249.4±2.6	0.283	48.01±0.92
3.	SLN-PEG1000-FA(SLNP1FA)	293.4±3.4	0.330	52.98±0.33
4.	SLN-PEG4000-FA(SLNP4FA)	315.0±3.4	0.385	58.22±0.51
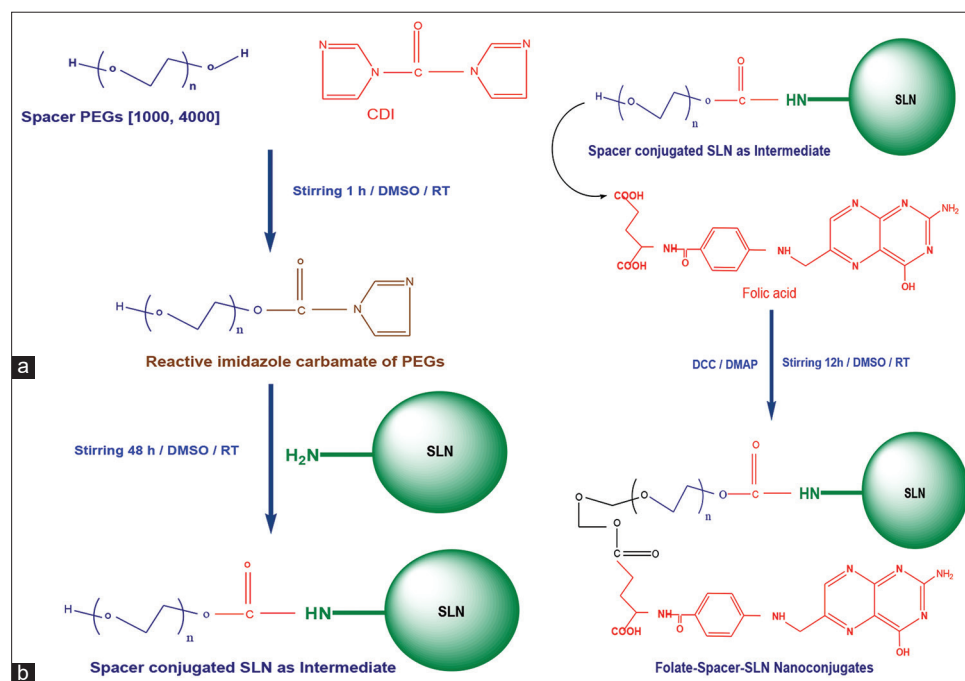
Scheme2: (a) Spacer nanoconjugates (b) Folate-spacer-solid lipid nanoparticles nanoconjugates
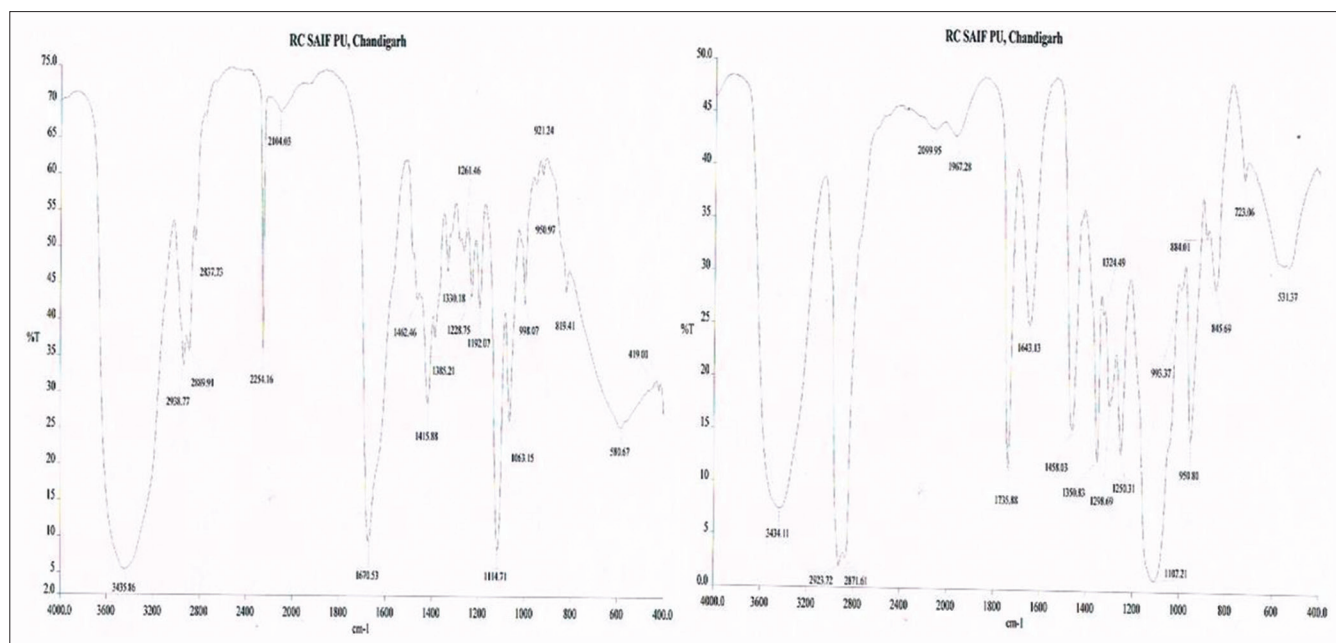
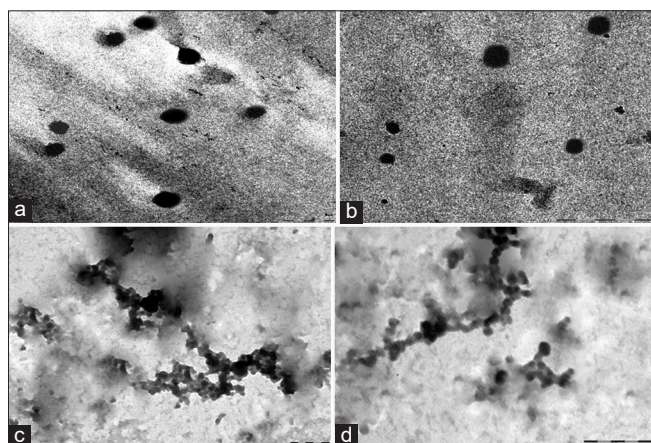**Fig. 1: Fourier-transform infrared spectrum of SLNP1FA and SLNP4FA**

Fig. 2: Transmission electron microscopic photograph of (a) plain solid lipid nanoparticles (SLNs) (b) coupled SLNs (c) SLNP1FA (d) SLNP4FA

Table 4: *In vitro* PTX release from different nanoformulations

Time (h)	% PTX release			
	SLN	SLNFA	SLNP1FA	SLNP4FA
1	18.28±1.36	15.81±3.01	8.88±2.23	5.29±1.81
2	31.12±2.1	24.01±1.32	26.08±1.17	18.28±0.82
3	43.28±1.71	33.89±3.12	28.18±1.37	23.1±1.34
4	52.12±1.09	44.08±3.08	36.22±2.01	29.94±2.19
5	65.82±2.88	53.09±0.97	46.81±3.16	40.91±1.71
6	77.89±1.92	67.08±1.8	61.3±2.44	57.46±2.43
8	88.14±2.78	77.19±2.07	63.9±1.88	55.82±1.69
12	96.39±1.56	86.08±2.27	80.19±0.97	76.06±1.3
24		91.08±0.99	89.28±3.14	83.07±1.49
36		97.84±1.43	97.12±0.99	96.28±1.03

Values represent mean± SD (n=3). PTX: Paclitaxel

drug content by measuring absorbance at 237 nm against blank [28] (Fig. 4, Table 4).

RESULTS AND DISCUSSION

Drug content and entrapment efficiency
Drug entrapment was determined by dialysis using a dialysis membrane and was found to be 79.3±0.5%. Keeping all optimization parameters under consideration, entrapment was found to be optimum in the selected formulation. A comparison was made between drug entrapment, surface morphology, particle size, and polydispersity index (PDI). Particle size (201.1±3.7 nm) of PTX loaded plain SLNs formulation was smaller than PTX loaded folate coupled SLNs and it was found to be 249.4±2.6 nm this may be due to formation of extra layer over the SLN surface due to the coating of folate on the surface of SLNs. PDI of plain formulations was also lower (PDI=0.234) than that of coupled formulation (PDI 0.283) this may be due to coupling of the SLN with the folate which disturbed the surface of the SLN. The drug entrapment efficiency of plain SLN was 79.3±0.5% which is more as compared to coupled SLN which having drug entrapment efficiency 71.7±0.5%, this may be because

of the leaching out the drug form the SLN during incubation period (Table 3).

FT-IR spectrum
In FT-IR spectrum of SLNP1FA and SLNP4FA, C-O stretch (ether linkage) strong, and sharp peak was obtained at 1114.71 cm^{-1} 1107.21 cm^{-1} due to polyether backbone of PEG, CH-NH-C(=O) amides bending peaks at 1462.46, 1415.88 cm^{-1}, and 1458.03 cm^{-1} due to amide bond formation between hydroxy group of PEG 1000 and 4000 and amine groups of SLN through CDI conjugation mechanism, Esters C-O stretching peaks at 1228.75, 1192.07 cm^{-1} and 1298.69, 1250.31 cm^{-1} confirmed the ester bond formation between the free hydroxy group of PEG 1000 and 4000 to carboxylic group of FA through DCC/DMAP conjugation protocol, and remaining peaks of aromatic compounds were indicated presence of FA (Fig. 1).

¹H NMR spectroscopy

The ¹H NMR spectrum and shifts of SLNFA as compared to that of simple SLNs furnish the proof of conjugation. In SLNFA newer peak of R-(C=O)-NH-CH$_2$-CH$_3$ of FA linkage appeared at 1.0–2.0 ppm. Similarly, SLNP1FA and SLNP4FA nanoconjugates exhibit characteristic peak of amide bond carbonyl proton and amide bond nitrogen proton appeared at 7.1–7.9 ppm and 3.0–3.4 ppm, and characteristic peak of ester bond formation between PEG and FA appeared at 3.7–4.1 ppm in contrast to SLN ¹H NMR spectrum [29] (Fig. 2).
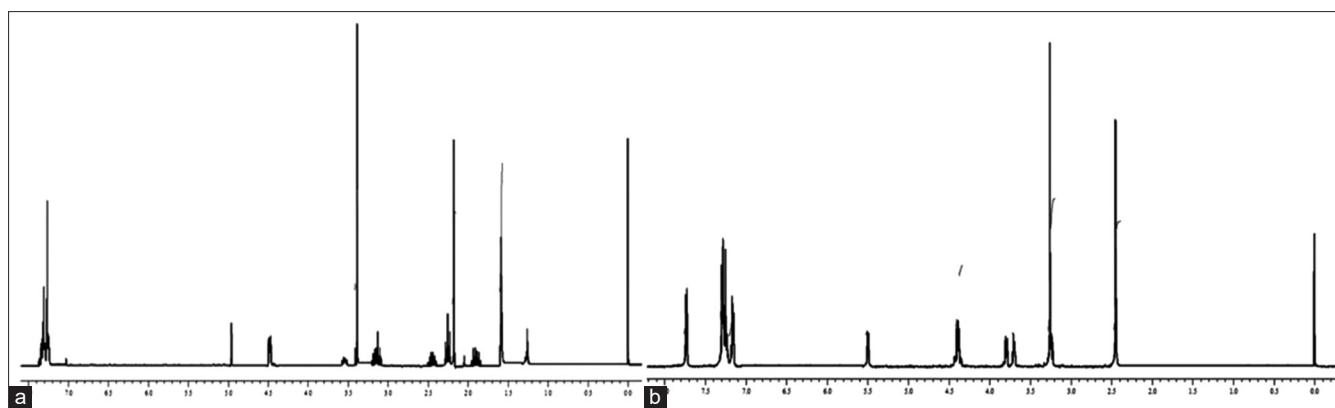
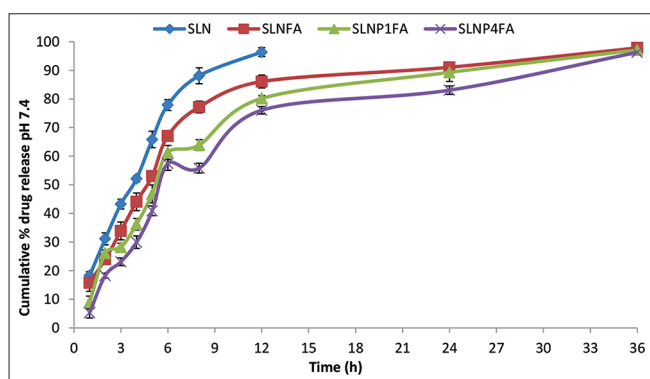Fig. 3: (a and b) ^{1}H NMR spectrum of SLNP1FA and SLNP4FA

Fig. 4: *In vitro* drug release profile of various nanoconjugates at pH 7.4

Table 5: Effect of storage on the particle size of plain and coupled SLNs at 4±1°C

Formulation code	Particle size (nm)			
	Initial	30 days	60 days	90 days
SLNs	201.1±3.5	204.1±2.4	208.2±1.3	209.5±4.2
SLNFA	249.4±3.4	256.3±2.1	258.7±4.6	274.4±3.7
SLNP1FA	293.4±2.5	300.5±3.1	320.8±4.1	335.6±3.5
SLNP4FA	315.0±1.3	324.9±3.2	334.3±4.9	340.4±2.6

formulations stored at 4±1°C, which indicates that the aggregation can be regulated by temperature and ideal storage condition being at 4±1°C.

The different SLN formulations were stored at 4±1°C and room temperature, and the percent of residual drug content was calculated after 30, 60, and 90 days by assuming the initial drug content to be 100%. Percent residual drug content of formulations was found to be 95.2±1.3% at 4±1°C and 90.3±2.4% at room temperature after 180 days in formulation plain SLN and 96.8±2.0% at 4±1°C and 93.4±2.1% at room temperature after 90 days in formulation coupled SLN. The residual drug content of formulations stored at room temperature was found to be lower in comparison to formulations stored at 4±1°C, which indicated that the formulations tend to degrade more at higher temper (Table 5).

3-(4,5-dimethylthiazol-2-yl)-2,5-diphenyltetrazolium bromide (MTT) cytotoxicity assay

The result of MTT assay was exhibited significant differences with various PTX nanoformulations. Plain PTX exhibited highest percent cell viability compared to PTX-loaded nanoformulations.(SLNFA, SLNP1FA, and SLNP4FA) on the *MCF-7* cell lines after 48 h of treatment. *MCF-7 cells* were seeded in 96 well micro plates and incubated for 48 h with various concentrations of samples ranging from 50 to 1600 nM. The percentage of cell death was estimated in term of percentage of cell viability. The percentage cell viability gradually decreased as the concentration of nanometric nanoformulations increased.

The result of the MTT assay exhibited significant differences with various PTX nanoformulations. Plain PTX exhibited highest percent cell viability compared to PTX loaded nanoformulations. Comparison of percentage cell viability for PTX loaded, SLNFA, SLNP1FA, and SLNP4FA showed the lowest percentage cell viability (highest percentage cell inhibition) for SLNP4FA in contrast with SLNFA and SLNP1FA. Based on obtained results of MTT assay, the percentage cell viability of SLNFA, SLNP1FA, and SLNP4FA did not show any definite correlation according to the conjugation of folate and PEGs as spacer up to the concentration of 100 nM. The percentage cell inhibition of nanoformulations at 400, 800, and 1600 nM can be ranked as follows (Fig. 5 and Table 6):

Microscopic study

The electron microscopic analysis of nanoconjugates proves them to be as nanometric sized vesicles, which was evident by TEM photograph. The data revealed the increase in particle size on folate conjugation, directly and through PEGs spacer (Fig. 3). The size of nanoconjugates slightly increased with molecular weight of PEGs and the order of size of nanoconjugate were found to be SLNP4FA> SLNP1FA> SLNFA> SLN.

Drug release study

The release of drug PTX from SLN nanoformulations was monitored by a dialysis method. The dialysis was carried out at 37°C using dialysis membranes with molecular weight cutoff of 10 kDa and phosphate-buffered saline (pH 7.4) as the sink solution. The concentration of drug was analyzed at various time points during the dialysis process to obtain the *in vitro* drug release profile. *In vitro* drug release data of PTX associated with nanoconjugates is presented in Fig. 4. Moreover, the release patterns of SLNP1FA and SLNP4FA were sustained with increasing chain length of PEGs (Mw: 1000, 4000) in both release conditions. This may be attributed to the surface engineering of folate and folate PEGs as it led to more sealing at the nanometric periphery and hydrophobic interactions, which delayed the drug release. The rate of drug release of nanoconjugates was observed to be low due to close structure and steric hindrances due to large chain length of PEGs as spacer. Hence, folate attachment through PEG's spacer on SLNs can be proposed for better sustained and controlled release drug delivery system (Table 4).

Stability testing

The storage stability testing indicated that plain SLN and coupled SLN formulations stored at 4±1°C were more stable than those stored at room temperature. Average particle size of nanoparticles was found to increases on storage, which can be due to the aggregation of particles at different storage conditions. This effect was least in the case of

SLNP4FA>SLNP1FA>SLNFA (vice versa for percentage cell viability).

However, all the formulations showed dose-dependent inhibition of *MCF-7* cells. The IC_{50} values of SLNFA, SLNP1FA, and SLNP4FA were undetectable up to the concentration of 200 nM. IC_{50} values of SLNFA, SLNP1FA, and SLNP4FA were found to be 403.08, 370.34, and 331.29 nm, respectively, and percentage reduction in IC_{50} of SLNFA, SLNP1FA, and SLNP4FA with respect to PTX was found to be 21.78925, 32.23422, and 48.39127, respectively (Table 9.3 and Fig. 9.3). SLNP4FA exhibited maximum percentage reduction in IC_{50}; hence, SLNP4FA had highest cytotoxicity and target ability among Folate-spacer (SLNP1FA, and SLNP4FA) and SLNFA (Table 7).

SLNP4FA was responsible for higher uptake and target ability due to receptor specific targeting of SLNs due to surface conjugation of FA through PEG (Mw: 4000) as spacer, folate enhanced the receptor mediated endocytosis of nanoformulations and PEGs used as a spacer to couple ligand (FA) moieties to surfaces of nanometric carrier thus potentially provide both "bioinert" and "bioactive" functions to nanoformulations. Based on obtained IC_{50} value of synthesized nanoconjugates arranged for target ability:

SLNP4FA>SLNP1FA>SLNFA.

Cell topographic study of PTX and PTX loaded nanoformulations (SLN, SLNFA, SLNP1FA, and SLNP4FA) were performed with a view to assess the ability of different drug loaded formulations to target human mammary carcinoma cells, *MCF-7* (Fig. 9.2 to 9.8). Similar to the results of the percent cell growth inhibition assay, cell topographic studies also displayed higher uptake of folate-spacer conjugated nanoformulations contrast with plain PTX and SLNFA (Fig. 6). The higher uptake was possibly due to the conjugation of folate through PEGs as spacer on the surface of the SLN as compared to direct conjugation of folate on the surface of the SLN. This might be due to higher drug loading, resulting in a higher release. Among SLNP1FA and SLNP4FA, the highest uptake was observed with the SLNP4FA because PEG (Mw: 4000) exhibits more tumor accumulation. The results support the strategy that optimized spacer chain length for effective tumor targeting can provide higher uptake of anticancer bioactive to the cancer cells [30].

This study is in agreement that the SLNFA and folate-spacer (SLNP1FA and SLNP4FA) nanometric nanoformulations entered into the cancer cell by receptor mediated endocytosis (folate receptors are overexpressed in *MCF-7* cell line). Singh *et al*. previously reported the direct and indirect conjugation of folate through one spacer (PEG Mw: 4000) on the surface of nanocarriers. This is the 1st time conjugation of folate directly and indirectly using two spacer (PEGs Mw: 1000 and 4000) with the SLN was performed and assessed the tumor targeting potential against *MCF-7* cell lines. *In vitro* MTT and cell uptake assay concluded that SLNP4FA bears significant tumor targeting potential as compared to free PTX and PTX loaded nanoformulations (SLNFA and SLNP1FA). Based on obtained results tumor targeting potential can be ranked as follows [31]:
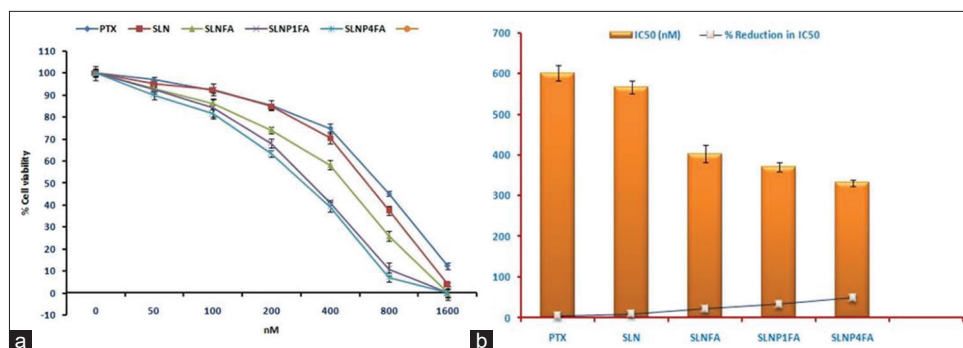
SLNP4FA>SLNP1FA>SLNFA.

Fig. 5: (a) % Cell viability in MCF-7 cells treated with plain paclitaxel (PTX) and PTX loaded nanoformulations. (b) Relative change in IC_{50} of MCF-7 cells with plain PTX and PTX loaded nanoformulations treatment

Fig. 6: Microscopic image of *MCF-7* cells (×40) and MCF-7 cells after 48 h with solid lipid nanoparticles (×40), paclitaxel (×40)

Table 6: % cell viability

Conc (nM)	0	50	200	400	800	1600
PTX	100±0.89	96.99±1.42	85.32±2.35	74.82±2.39	45.18±1.23	12.34±1.45
SLN	100±1.88	95.12±1.39	84.87±1.43	70.56±2.57	37.48±2.22	3.82±0.91
SLNFA	100±3.26	93.01±1.67	74.06±1.4	58.21±2.02	25.89±2.24	0±2.19
SLNP1FA	100±1.52	92.45±1.81	68.13±1.9	41.11±1.19	10.91±3.02	0±1.87
SLNP4FA	100±1.12	90.07±1.91	63.45±1.54	39.32±2.24	7.12±2.11	0±3.14

PTX: Paclitaxel

Table 7: IC$_{50}$ of PTX loaded nano formulations and % reduction in IC$_{50}$ with respect to plain PTX

Nanoconjugates	IC$_{50}$ (nM)	% Reduction in IC$_{50}$
PTX	601.18±19.22	4.998149
SLN	567.45±15.26	9.008761
SLNFA	403.08±21.09	21.78925
SLNP1FA	370.34±10.91	32.23422
SLNP4FA	331.29±7.01	48.39127

SD (n=3). PTX: Paclitaxel

CONCLUSION

Engineering of the dendritic surface with targeting ligand such as FA can enhance the site specific anticancer drug delivery. PEGylation of SLN can improve the circulation time of SLN in the body. In the present study, combination of both of these approaches displayed promising results in terms of tumor-targeting potential. The present study was aimed to developed surface-engineered SLN by conjugation of folate directly or indirectly through different types of PEGs (Mw: 1000, and 4000) as spacers with more biocompatibility and less toxicity, but at the same time, the ability to deliver drug at the desired site of action. The reduced toxicity and enhanced tumor-targeting potential with SLN4FA can be used most suitably as a controlled and targeted drug delivery system for the delivery of anticancer drugs like PTX. The nanoformulations can be given through the intravenous route as a long-term circulatory nanoparticulate system. This is a debut study reporting FA conjugation to the surface through four PEGs as spacer and optimized the spacer chain length for effective cancer targeting through SLN. This report as a whole is believed to shed new light on the role of spacer chain length in targeting potential of folate-anchored SLN.

ACKNOWLEDGMENTS

CONFLICT OF INTEREST

The authors declare that they have no conflict of interest.

REFERENCES

1. Smith RD, Mallath MK. History of the growing burden of cancer in India: From antiquity to the 21st century. J Glob Oncol 2019;5:1-15.
2. Shaikh FY, Gills JJ, Sears CL. Impact of the microbiome on checkpoint inhibitor treatment in patients with non-small cell lung cancer and melanoma. EBioMedicine 2019;48:642-7.
3. Bardot J, Magalon G, Mazzola RF. History of breast cancer reconstruction treatment. Ann Chir Plast Esthet 2018;63:363-9.
4. Lemjabbar-Alaoui H, Hassan OU, Yang YW, Buchanan P. Lung cancer: Biology and treatment options. Biochim Biophys Acta 2015;1856:189-210.
5. Minassian LM, Cotechini T, Huitema E, Graham CH. Hypoxia-induced resistance to chemotherapy in cancer. Adv Exp Med Biol 2019;1136:123-39.
6. Hirsch FR, Scagliotti GV, Mulshine JL, Kwon R, Curran WJ Jr., Wu YL, *et al*. Lung cancer: Current therapies and new targeted treatments. Lancet 2017;389:299-311.
7. Maeda H. The link between infection and cancer: Tumor vasculature, free radicals, and drug delivery to tumors via the EPR effect. Cancer Sci 2013;104:779-89.
8. Alimoradi H, Matikonda SS, Gamble AB, Giles GI, Greish K. Hypoxia responsive drug delivery systems in tumor therapy. Curr Pharm Des 2016;22:2808-20.
9. Durymanov MO, Rosenkranz AA, Sobolev AS. Current approaches for improving intratumoral accumulation and distribution of nanomedicines. Theranostics 2015;5:1007-20.
10. Nakamura H, Fang J, Maeda H. Development of next-generation macromolecular drugs based on the EPR effect: Challenges and pitfalls. Expert Opin Drug Deliv 2015;12:53-64.
11. Chang J, Paillard A, Passirani C, Morille M, Benoit JP, Betbeder D, *et al*. Transferrin adsorption onto PLGA nanoparticles governs their interaction with biological systems from blood circulation to brain cancer cells. Pharm Res 2012;29:1495-505.
12. Maeda H, Nakamura H, Fang J. The EPR effect for macromolecular drug delivery to solid tumors: Improvement of tumor uptake, lowering of systemic toxicity, and distinct tumor imaging *in vivo*. Adv Drug Deliv Rev 2013;65:71-9.
13. Rehman M, Ihsan A, Madni A, Bajwa SZ, Shi D, Webster TJ, *et al*. Solid lipid nanoparticles for thermoresponsive targeting: Evidence from spectrophotometry, electrochemical, and cytotoxicity studies. Int J Nanomedicine 2017;12:8325-36.
14. Paliwal R, Paliwal SR, Kenwat R, Kurmi BD, Sahu MK. Solid lipid nanoparticles: A review on recent perspectives and patents. Expert Opin Ther Pat 2020;30:179-94.
15. Tapeinos C, Battaglini M, Ciofani G. Advances in the design of solid lipid nanoparticles and nanostructured lipid carriers for targeting brain diseases. J Control Release 2017;264:306-32.
16. Miglietta A, Cavalli R, Bocca C, Gabriel L, Gasco MR. Cellular uptake and cytotoxicity of solid lipid nanospheres (SLN) incorporating doxorubicin or paclitaxel. Int J Pharm 2000;210:61-7.
17. Cassano R, Ferrarelli T, Mauro MV, Cavalcanti P, Picci N, Trombino S. Preparation, characterization and *in vitro* activities evaluation of solid lipid nanoparticles based on PEG-40 stearate for antifungal drugs vaginal delivery. Drug Deliv 2016;23:1047-56.
18. Gonçalves LM, Maestrelli F, di Cesare Mannelli L, Ghelardini C, Almeida AJ, Mura P. Development of solid lipid nanoparticles as carriers for improving oral bioavailability of glibenclamide. Eur J Pharm Biopharm 2016;102:41-50.
19. Conte C, Fotticchia I, Tirino P, Moret F, Pagano B, Gref R, *et al*. Cyclodextrin-assisted assembly of PEGylated polyester nanoparticles decorated with folate. Colloids Surf B Biointerfaces 2016;141:148-57.
20. Alshubaily FA. Enhanced antimycotic activity of nanoconjugates from fungal chitosan and Saussurea costus extract against resistant pathogenic Candida strains. Int J Biol Macromol 2019;141:499-503.
21. Rosière R. New folate-grafted chitosan derivative to improve delivery of paclitaxel-loaded solid lipid nanoparticles for lung tumor therapy by inhalation. Mol Pharm 2018;15:899-910.
22. Kanwar R, Gradzielski M. Biomimetic solid lipid nanoparticles of sophorolipids designed for antileprosy drugs. J Phys Chem B 2018;122:6837-45.
23. Malekpour-Galoghahi F, Hatamian-Zarmi A, Ganji F, Ebrahimi-Hosseinzadeh B, Nojoki F, Sahraeian R, *et al*. Preparation and optimization of rivastigmine-loaded tocopherol succinate-based solid lipid nanoparticles. J Liposome Res 2018;28:226-35.
24. Rajpoot K, Jain SK. Colorectal cancer-targeted delivery of oxaliplatin via folic acid-grafted solid lipid nanoparticles: Preparation, optimization, and *in vitro* evaluation. Artif Cells Nanomed Biotechnol 2018;46:1236-47.
25. Pawar H, Surapaneni SK, Tikoo K, Singh C, Burman R, Gill MS, *et al*. Folic acid functionalized long-circulating co-encapsulated docetaxel and curcumin solid lipid nanoparticles: *In vitro* evaluation, pharmacokinetic and biodistribution in rats. Drug Deliv 2016;23:1453-68.
26. Thambiraj S, Shruthi S, Vijayalakshmi R, Shankaran DR. Evaluation of cytotoxic activity of docetaxel loaded gold nanoparticles for lung cancer drug delivery. Cancer Treat Res Commun 2019;21:100157.
27. Hami Z, Rezayat SM, Gilani K, Amini M, Ghazi-Khansari M. *In vitro* cytotoxicity and combination effects of the docetaxel-conjugated and doxorubicin-conjugated poly (lactic acid)-poly (ethylene glycol)-folate-based polymeric micelles in human ovarian cancer cells. J Pharm Pharmacol 2017;69:151-60.
28. Saha S, Bhattacharjee A, Rahaman SH, Basu A, Chakraborty J. Synergistic anti-cancer activity of etoposide drug loaded calcium aluminium layered double hydroxide nanoconjugate for possible application in non small cell lung carcinoma. Appl Clay Sci 2020;188:105496.
29. Kumar CS, Thangam R, Mary SA, Kannan PR, Arun G, Madhan B. Targeted delivery and apoptosis induction of trans-resveratrol-ferulic acid loaded chitosan coated folic acid conjugate solid lipid nanoparticles in colon cancer cells. Carbohydr Polym 2020;231:115682.
30. Popat A, Karmakar S, Jambhrunkar S, Xu C, Yu C. Curcumin-cyclodextrin encapsulated chitosan nanoconjugates with enhanced solubility and cell cytotoxicity. Colloids Surf B Biointerfaces 2014;117:520-7.
31. Wang W, Zhou F, Ge L, Liu X, Kong F. A promising targeted gene delivery system: Folate-modified dexamethasone-conjugated solid lipid nanoparticles. Pharm Biol 2014;52:1039-44.